Journal of the European Ceramic Society 15 (1995) 1025–1029

0955-2219(95)00068-2
0955-2219/95/$9.50

Thermal Properties and Devitrification Behaviour of $(2-x)CaO \cdot x/3Y_2O_3 \cdot 2SiO_2$ Glasses

A. Costantini, F. Branda & A. Buri

Dipartimento di Ingegneria dei Materiali e della Produzione, Università de Napoli 'Federico II', 80125 Napoli, Italy

(Received 23 July 1993; revised version received 7 March 1995; accepted 20 March 1995)

Abstract

The thermal properties (glass transformation, T_g, softening, T_s, and exo-peak, T_p, temperatures), and the devitrification behaviour of glasses in the system $CaO–Y_2O_3–SiO_2$ are reported. The T_g, T_p and E_c results can be explained on the basis of the increased structural rigidity when Ca^{+2} ions are substituted by Y^{+3} ions, with the formation of stronger bonds to the oxygen.

For the molar ratio of Ca/Si = 0·7 or more, wollastonite is no longer formed; at the same time a new and as yet unidentified phase appears. Surface nucleation occurs preferentially, but, in finely powdered samples, which soften and sinter before devitrifying, surface nuclei behave virtually as bulk nuclei.

Introduction

In this paper the thermal properties and the study of the devitrification behaviour of glasses of the system $CaO–Y_2O_3–SiO_2$ are reported. In particular the effect of the substitution of Y_2O_3 to CaO in a glass of composition $CaO–SiO_2$ (wollastonite) has been studied.

The devitrification process has been studied by differential thermal analysis (DTA).

CaO and SiO_2 in a molar ratio $CaO/SiO_2 \simeq 1$ are the basic components of bioactive glasses and glass-ceramics.[1,2] Otherwise it is known that the addition of yttrium oxide to silicates allows us to obtain glasses with high elastic moduli and hardness.[3] The addition of Y_2O_3 has proved to be useful in also obtaining glass-ceramics which have interesting properties. Machinable glass ceramics have been obtained in the system $CaO–Al_2O_3–Y_2O_3–SiO_2$.[4] Refractory glasses have been obtained in the system $Y_2O_3–Al_2O_3–SiO_2$.[5]

The non-isothermal devitrification of glasses in this system is interesting because, in the temperature range of efficient devitrification, powder sintering occurs. As will be shown, this has consequences on the devitrification mechanism.

Experimental

Glasses of composition expressed by the following formula

$$(2-x)CaO.(x/3)Y_2O_3.2SiO_2 \text{ where } 0 \leq x \leq 1{\cdot}0$$

were prepared by melting analytical grade reagents, Y_2O_3, $CaCO_3$ and SiO_2 in a platinum crucible in an electric furnace for 4 h, in the temperature range 1400–1600°C. The melts were quenched by plunging the bottom of the crucible into cold water.

Differential thermal analysis (DTA) was carried out by means of a Netzsch Differential Scanning Calorimeter (DSC) model 404M on about 50 mg powdered samples at various heating rates (2–20°C/min). Fine (63–90 μm) and coarse (500–315 μm) powdered samples were used. Powdered Al_2O_3 was used as reference material.

Devitrified samples were analyzed by computer-interfaced X-ray (CuKα) powder diffractometry (XRD) using a Philips Diffractometer model PW1710, with a scan speed of 1°min^{-1} and a built-in computer search program. The crystalline phases were identified by means of JCPDS cards.

Results

The DTA curves of the studied glasses, together with the derivative curve (DDTA) for one of them, are reported in Figs 1 and 2 as recorded at 10°C/min heating rate; the data are for fine, (63–90 μm), (Fig. 1) and coarse, (315–500 μm), (Fig. 2) powdered samples. When a glass is heated in a DTA apparatus a slope change appears on the recorded curve when passing through the glass transformation temperature range. The glass transformation temperature, T_g, has been taken from the derivative curve as indicated in Fig. 1.

As can be seen in many cases, the first slope change in the glass transformation range is followed by a second one at a temperature lower than the onset of the devitrification exo-peak.

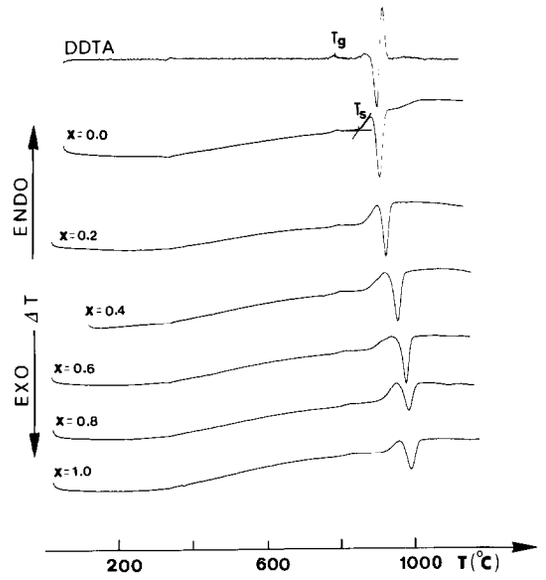

Fig. 1. DTA and DDTA curves recorded at 10°C/min heating rate on fine (63–90 μm) powdered samples.

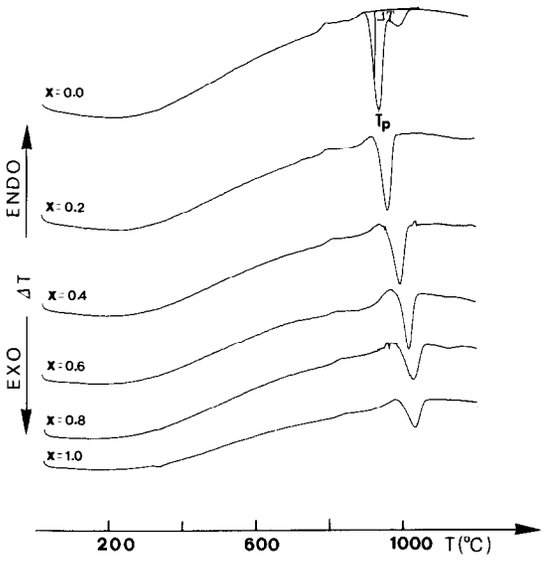

Fig. 2. DTA curves recorded at 10°C/min heating rate on coarse (315–500 μm) powdered samples.

As a matter of fact in these cases the initially powdered samples were recovered from the DTA sample holder as porous bodies. Therefore the second slope change is to be linked to the change in the thermal exchange coefficients when powders soften and sinter. The effect is much more pronounced in the case of the fine powders. The softening temperatures can be taken from the DTA curves as indicated in Fig. 1.

In Figs 3, 4 and 5 the glass transformation, T_g, softening, T_s, and DTA exo-peak, T_p, temperatures are reported as a function of composition. In Table 1 the values of the onset and peak temperatures of the devitrification exo-peaks are reported. As can be seen, all of them increase as the Y_2O_3 content is increased.

In Fig. 6 the X-ray diffraction patterns are

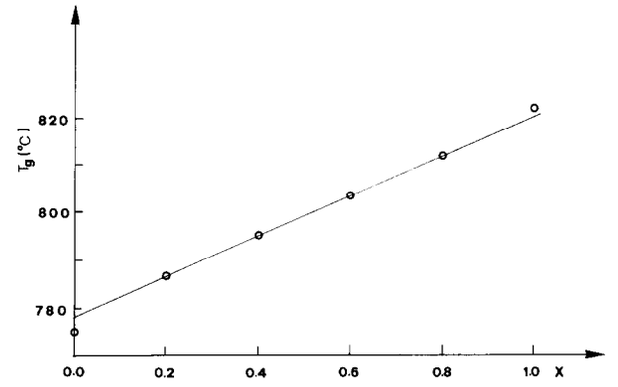

Fig. 3. Plot of the glass transformation temperature T_g versus composition.

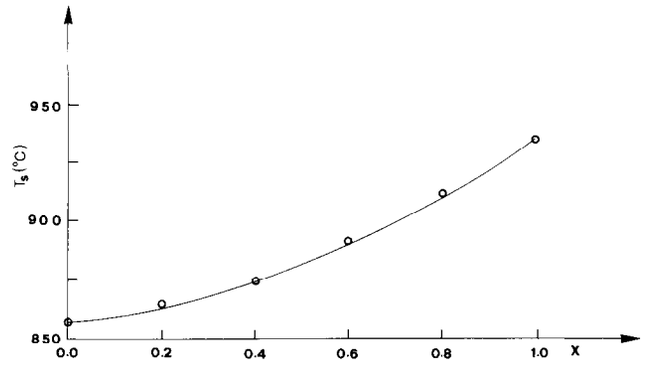

Fig. 4. Plot of the softening temperature T_s versus composition.

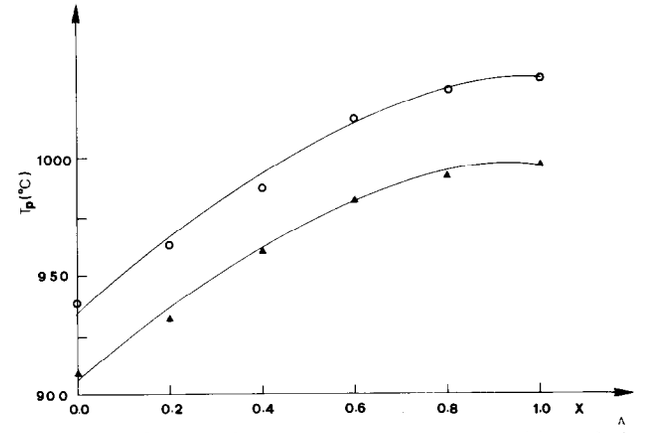

Fig. 5. Plot of exo-peak temperature versus composition relative to fine powdered (▲) and coarse powdered (○) samples.

Table 1. Onset and peak temperature of devitrification exo-peaks relative to fine (T_{of}, T_{pf}) and coarse (T_{oc}, T_{pc}) powders

Composition	T_{of}(°C)	T_{pf}(°C)	T_{oc}(°C)	T_{pc}(°C)
$x = 0$	880	910	895	940
$x = 0{\cdot}2$	903	929	918	962
$x = 0{\cdot}4$	926	962	938	993
$x = 0{\cdot}6$	945	984	970	1018
$x = 0{\cdot}8$	961	991	985	1028
$x = 1{\cdot}0$	970	997	990	1034

reported relative to the pattern of a sample submitted to a DTA run which was stopped just after the exo-peak. As can be seen in the (a)–(d) patterns, the lines of wollastonite (JCPDS card

29/372) appear, but their intensity progressively reduces as the Y_2O_3 is substituted for CaO. In the (b) and (c) patterns the lines of pseudo-wollastonite, CaO.SiO_2, (JCPDS card 19/248) are also present. In the (c) pattern another, unidentified, phase appears, whose lines progressively substitute those of wollastonite phase.

In Table 2 the *d*-spacings' values and relative intensity of the lines of the unknown phase are reported.

The non-isothermal devitrification was also studied. The kinetic parameters were determined by using the following two equations:

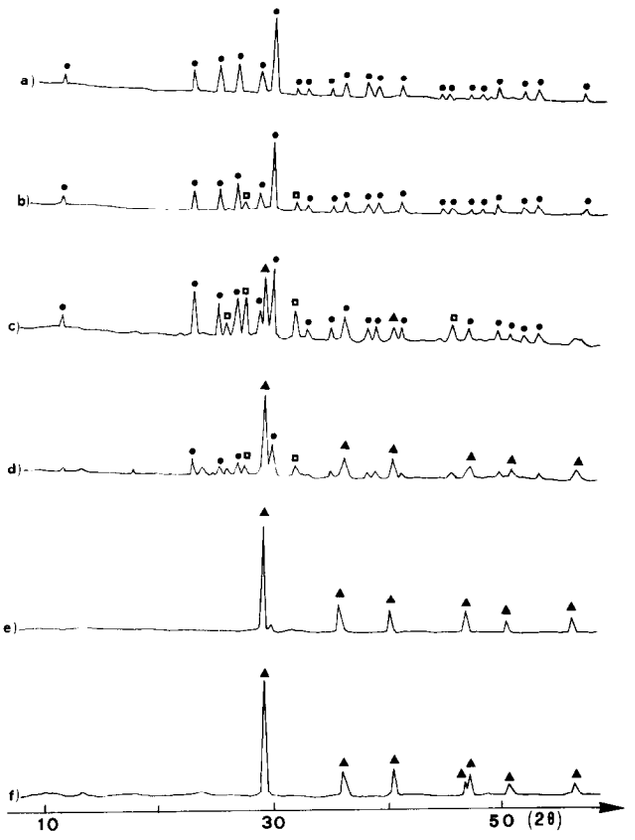

Fig. 6. X-ray diffraction patterns of samples devitrified during a DTA run: (a) $x = 0$; (b) $x = 0{\cdot}2$; (c) $x = 0{\cdot}4$; (d) $x = 0{\cdot}6$; (e) $x = 0{\cdot}8$; (f) $x = 1{\cdot}0$. (●) wollastonite (JCPDS card 29/372); (□) pseudowollastonite (JCPDS card 19/248); (▲) unknown phase.

Table 2. *d*-spacings and relative intensity of the lines of diffraction pattern of Fig. 6(f) that have not been attributed (S = strong; W = weak)

Unknown phase Distance plane (A)	*Relative intensity*
3·045	S
2·494	W
2·487	W
2·222	W
1·931	WW
1·920	W
1·631	WW
1·626	WW

$$\ln\beta = -E_c/RT_p + \text{const} \quad (1)$$

$$\ln \Delta T = -mE_c/RT + \text{const} \quad (2)$$

Eqns 1 and 2 can be derived from the well known following eqn:[6,7]

$$-\ln(1 - \alpha) = (AN/\beta^m)\exp(-mE_c/RT) \quad (3)$$

where α is the crystallization degree, N is the nuclei number and A is a constant, β is the heating rate, ΔT and T_p the deflection from the base line and the peak temperature taken as indicated in Fig. 2 and T is the temperature. As in inorganic glasses, the devitrification exo-peak occurs in a temperature range higher than that of efficient nucleation,[6] E_c is the crystal growth activation energy. The parameter m depends upon the mechanism and morphology of crystal growth; it ranges from $m = 1$ for 1-dimensional growth (or growth from surface nuclei) to $m = 3$ for 3-dimensional growth.[6,7]

Eqns 1 and 2 can be derived from it by supposing: (1) α at peak temperature is not dependent on the heating rate;[8] (2) ΔT is proportional to the instantaneous reaction rate:[9,10] and (3) in the initial part of the DTA crystallization peak, the change in the temperature has a much lower effect than α on the T.[11]

In Fig. 7 the plots of $\ln\beta$ versus $1/T_p$ are reported for the fine powdered samples. In Figs 8 and 9 the plots of $\ln\Delta T$ versus $1/T$ are reported for fine and coarse powdered samples taken from DTA curves recorded at 10°C/min. According to eqns 1 and 2, straight lines were obtained. Their slopes allow, therefore, to evaluate the E_c and mE_c

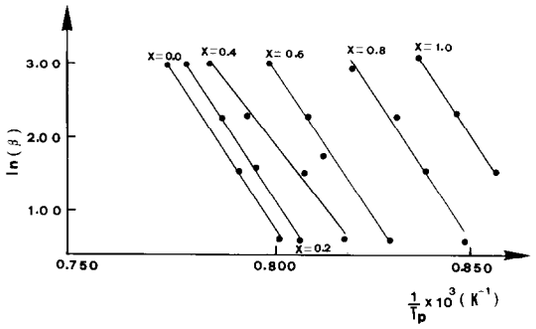

Fig. 7. Plot of $\ln\beta$ versus $1/T_p$.

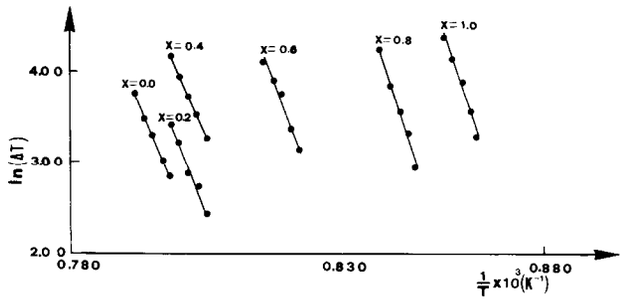

Fig. 8. Plot of $\ln\Delta T$ versus $1/T$ relative to fine powered samples (63–90 μm).

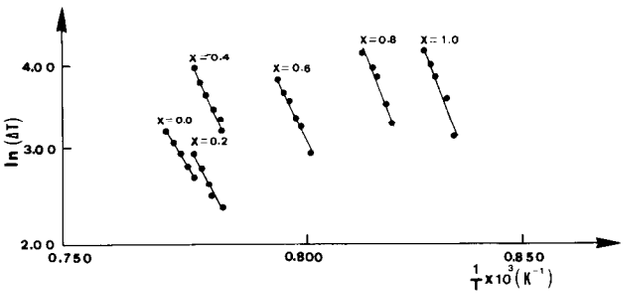

Fig. 9. Plot of ln ΔT versus $1/T$ relative to coarse powdered samples (315–500 μm).

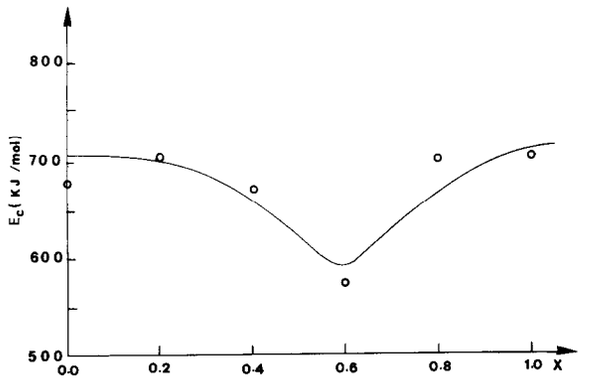

Fig. 10. Plot of the activation energy for crystalline growth E_c versus composition.

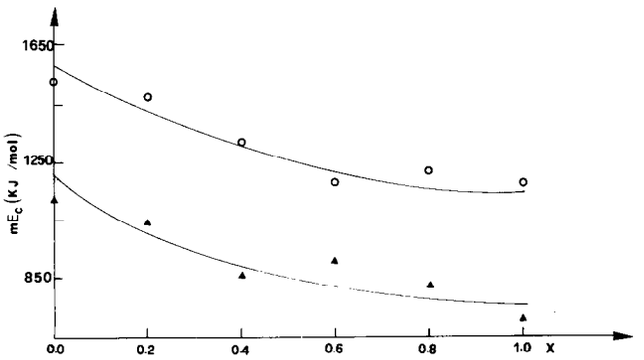

Fig. 11. Plot of the mE_c values versus composition relative to fine powdered samples (63–90 μm). (○) and coarse powdered samples (315–500 μm) (▲).

values reported in Figs 10 and 11. The curve of E_c versus composition shows a minimum. As can be seen in Fig. 11, for each glass, the mE_c values appear to increase as the specific surface of the samples is increased. When comparing the values of E_c with the mE_c relative to fine powdered samples, values of $m \approx 2$ are obtained for all glasses of the studied system. In the case of coarse powdered samples values $1 \leq m \leq 2$ are always obtained.

Discussion

The increase of T_g as the Y_2O_3 is substituted to CaO can be explained by taking into account that, according to Ray,[12] the glass transformation temperature depends on the density of covalent cross-linking and the number and strength of the cross-links between the cation and oxygen atoms. It's worth remembering that CaO and Y_2O_3 are reported to be modifier oxides;[13] therefore, in the studied series, the density of covalent cross-linking doesn't change because the molar ratio O/Si is constant. When this happens, it was found that the changes of T_g when a modifier oxide is substituted for another one can be related to their coordination number and strength of bonds to oxygen atoms, linked to the field strength Z/r^2, where Z is the charge and r the radius of the cation.[13] Ca^{+2} and Y^{+3} have the same coordination number in their pure oxide structures;[13] otherwise Y^{+3} has a greater field strength (3·76 A–2 instead of 2·04 A–2) and a greater single bond strength in the pure oxide structure (210 KJ/mol instead of 130 KJ/mol.[13]) The T_g increase can therefore be ascribed to the greater strength of the cross-links between the Y^{+3} cation and oxygen atoms.

With this in mind we can also find an explanation for the increasing trend of the T_p curve.

In Fig. 10, it must be taken into account that the crystal growth activation energy, E_η, is usually equal to the viscous flow activation energy, E_η,[14] the viscosity depends upon the temperature according to the VFT equation,[15] which implies that E_η continuously decreases as the temperature increases:

$$\log\eta = A + B/(T-To)$$

where η is the viscosity, T is the temperature, A, B and To are constants whose values depend on the glass composition.

Otherwise E_η should increase as Y_2O_3 is substituted to CaO, as long as this involves the structure rigidity being increased, as discussed earlier. The trend in Fig. 10 gives an explanation for these 'temperature' and 'compositional' effects. Therefore, initially the 'temperature' effect could overwhelm the 'compositional' one, which should become dominant starting from x = 0·6. In fact, Table 1 shows that until x = 0·6, a continuous increase of T_p is observed; the maximum difference being as great as 80°C. Figure 5 shows that when x = 0·6 the slope of the T_p/x plot changes and the 'compositional' effect can became dominant.

XRD results (Fig. 6) indicate that, in the presence of Y_2O_3, starting from the molar ratio Ca/Si = 0·7 (x = 0·6), more wollastonite does not form; at the same time a new phase appears that is not reported on the JCPDS cards.

The mE_c values appear to increase as the

specific surface of the samples is increased. Usually the opposite result is obtained owing to the fact that the greater the specific surface, the greater the tendency to devitrify by growth from surface nuclei so that m is progressively reduced to the value $m = 1$. In the case of diopside glass[16] it was found that nucleation preferentially occurs at the surface of the sample, but surface nuclei formed in the glass transformation range behave as bulk nuclei in finely powdered samples that efficiently sinter before devitrifying. This hypothesis appears to be effective in explaining the devitrification behaviour of all the studied glasses. In fact in the case of coarse powdered samples that sinter badly (see Figs 1 and 2), a value $1 \leq m \leq 2$ were obtained. On the contrary, in the case of finely powdered samples that sinter well before devitrifying, higher values of the m parameter have been obtained. The value $m \approx 2$ for wollastonite agrees with the reported result that its crystals are often in the form of tablets.[17]

Conclusions

The following conclusions can be drawn from the experimental results:

(1) T_g, T_p, and E_c results suggest that the substitution of Y_2O_3 for CaO causes the structure rigidity to increase.

(2) Starting from the molar ratio Ca/Si = 0·7, more wollastonite does not form; at the same time a new phase appears that is not reported on the JCPDS cards.

(3) The homogeneous nucleation rates are very low; nevertheless surface nuclei can behave as bulk nuclei in powdered samples that sinter before devitrifying. In this case values $m \approx 2$ were found for all the studied glasses.

References

1. Hench, L. L., Bioceramics: from concept to clinic. *J. Am. Cer. Soc.*, **74**(7) (1991) 1487–510.
2. Kokubo, T., Novel bioactive materials derived from glasses. Proc. XVI International Congress on Glass, Madrid, Vol. 1, *Bol. Soc. Esp. Ceram. Vid.*, **31-C1** (1992) 119–37.
3. Makishima, A., Tamura, Y. & Sakaino, T., Elastic moduli and refractive indices of aluminosilicate glasses containing Y_2O_3, La_2O_3 and TiO_2, *J. Am. Cer. Soc.*, **61**(5–6) (1978) 247.
4. Makishima, A., Asami, M. & Ogura, Y., A machinable calcia–alumina–yttria–silica glass-ceramic, *J. Am. Cer. Soc.*, **72**(6) (1989) 1024.
5. Arita, I., Wilkinson, D. & Purdy, G., Crystallization of yttria-alumina–silica glasses, *J. Am. Cer. Soc.*, **75**(12) (1992) 3315.
6. Matusita, K. & Sakka, S., Kinetic study of non-isothermal crystallization of glass by thermal analysis, *Bull. Inst. Chem. Res. Kyoto Univ.*, **59** (1981) 159–71.
7. MacFarlane, D. R., Matecki, M. & Poulain, M., Crystallization in fluoride glasses devitrification on reheating. *J. Non-Cryst. Solids*, **64** (1984) 351–62.
8. Boswell, P. G., On the calculation of activation energies using a modified Kissinger method. *J. Thermal Anal.*, **18** (1980) 353–8.
9. Borchardt, H. J. & Daniels, F., The application of differential thermal analysis to the study of reaction kinetics. *J. Am. Chem. Soc.*, **79** (1957) 41–6.
10. Akita, K. & Kase, M., Relationship between the DTA peak and the maximum reaction rate. *J. Phys. Chem.*, **72** (1968) 906–13.
11. Piloyan, F. O., Ryabchica, I. V. & Novikova, O. S., Determination of activation energies of chemical reactions by differential thermal analysis. *Nature*, **212** (1966) 1229.
12. Ray, N. H., Composition-property relationships in inorganic oxide glasses. *J. Non-Cryst. Solids*, **15** (1974) 423–34.
13. Rawson, H., Inorganic glass forming systems. Academic Press, London & New York, 1967 pp. 24–5.
14. Matusita, K. & Sakka, S., Kinetic study on crystallization of glass by differential thermal analysis — criterion on application of Kissinger plot. *J. Non-Cryst. Solids*, **38–39** (1980) 741–6.
15. Scholze, H. (ed.). *Le Verre*, Institut du Verre, Paris, 1980, p. 69.
16. Branda, F., Costantini, A. & Buri, A., Non-isothermal devitrification behaviour of diopside glass. *Thermochim. Acta*, **217** (1993) 207–12.
17. Winchell, A. N. & Winchell, H., The microscopical characters of artificial inorganic substances: optical properties of artificial minerals, Academic Press New York and London, 1964, p. 291.